European Journal of Pharmaceutical Sciences 150 (2020) 105371

Contents lists available at ScienceDirect

European Journal of Pharmaceutical Sciences

journal homepage: www.elsevier.com/locate/ejps

Schiff bases of 4-Phenyl-2-Aminothiazoles as hits to new antischistosomals: Synthesis, *in vitro, in vivo* and *in silico* studies

Carina R. Amorim[a], Thais F.A. Pavani[a], Andrey F.S. Lopes[a], Marcelo D. Duque[a], Ana C.A. Mengarda[b], Marcos P. Silva[b], Josué de Moraes[b], Daniela G.G. Rando[a,*]

[a] *Departamento de Ciências Farmacêuticas, Instituto de Ciências Ambientais, Químicas e Farmacêuticas da Universidade Federal de São Paulo, UNIFESP, Rua São Nicolau, 210, Centro, Diadema, SP, Brasil*

[b] *Núcleo de Pesquisas em Doenças Negligenciadas da Universidade Guarulhos, Praça Teresa Cristina, 88, Guarulhos, SP, Brasil*

ARTICLE INFO

Keywords:
4-Phenyl-2-aminothiazoles
Schistosoma mansoni
Schiff bases
Antischistosomal
Target fishing

ABSTRACT

The treatment of schistosomiasis is based on a single drug, the praziquantel (PZQ), an oral bioavailable and efficient agent which causes minimal side effects. The main concern about this approach, however, is that relying on only one drug to treat a helminthic disease is a dangerous strategy since history shows that pathogens easily evolve to resistant forms. Actually, reports about experimental strains exhibiting low sensibility to PZQ can be found in literature. The search for new antischistosomals, consequently, is urgent. Here we report the synthesis of seventeen Schiff bases of 4-(4-Substituted phenyl)-N-(4-substituted benzylidene)thiazole-2-amines which were tested *in vitro* and *in vivo* against *Schistosoma mansoni* adult worms. Moreover, *in silico* studies to propose potential macromolecular targets and to predict the oral bioavailability were also performed. The analog GPQF-108 exhibited the best *in vitro* performance (IC_{50}: 29.4 μM, SI:6.1) associated with promising *in vivo* activity, with a significant decrease in the adult life forms and oviposition. Oral bioavailability could be impaired by the predicted low water solubility of GPQF-108, although it also exhibited good membrane permeability. The water solubility, however, could be improved by decreasing the particles size. Serine/Threonine- and Tyrosine Kinases, Carbonic Anhydrase, Tyrosine Phosphatase and Arginase were predicted as potential macromolecular targets through which the GPQF-108 could be acting against the helminth. This class of compounds exhibited an interesting initial therapeutic profile with the advantage of being chemically diverse from the PZQ and be easily synthesized from commercial reagents which could lead to low-cost drugs. These aspects make this class of compounds interesting hits to be explored against schistosomiasis.

1. Introduction

Schistosomiasis is a flatworm-caused disease responsible for 250 million cases worldwide, being 700 to 800 million people at risk of infection. Commonly associated with poverty, schistosomiasis occurs mainly in tropical and sub-tropical areas, most of the cases reported only in Africa. The etiological agents are helminths from *Schistosoma* genus, of which six are known to be human-pathogenic species (McManus et al., 2018).

The most prevalent species are the *S. mansoni*, endemic in sub-Saharan Africa and in Central-South American countries such as Suriname, Venezuela and Brazil, and the *S. haematobium*, prevalent in 54 countries of sub-Saharan Africa and Middle East (World Health Organization 2019).

The pharmacological treatment for schistosomiasis is based on the pyrazino-isoquinoline drug praziquantel. Commonly administered as tablets of 600 mg (40-60 mg/kg), this drug is effective against the adult worms, exhibiting minimal temporary side effects. For these reasons, the praziquantel has been considered a safe and efficient drug for more than 40 years (Lago et al., 2018).

Important, however, is the fact that relying on one single drug to treat a parasitic disease could lead to selection for resistance (Cioli et al., 2014). There are no evidence for widespread praziquantel resistance but reports of experimental isolates exhibiting diminished susceptibility to the drug as well as case reports about failures in treatment can easily be found in literature (Fenwick and Webster, 2006; Gryseels et al., 2001).

The loss of effectiveness of praziquantel could lead to a step back in the control of this helminthiasis and, for this reason, search for new therapeutic alternatives is urgent.

* Corresponding author.
E-mail address: dgrando@unifesp.br (D.G.G. Rando).

https://doi.org/10.1016/j.ejps.2020.105371
Received 20 February 2020; Received in revised form 13 April 2020; Accepted 30 April 2020
Available online 07 May 2020

In the last years, our group have been screening classes of chemical compounds, preferably those chemically diverse from Praziquantel (PZQ), to their antischistosomal activity. Among the assayed chemical classes, the Schiff bases from *N*-acylhydrazones and from 4-phenyl-2-aminothiazoles exhibited the best biological activities. The purpose is to explore different chemical scaffolds as starting points to be rationally optimized in the search for alternatives to antischistosomal therapy since this still relies in only one drug.

Schiff bases from 4-phenyl-2-aminothiazoles have been explored for several potential biological applications such as antibacterial, antifungal, antitumoral, anti-inflammatory, antitubercular activities (Brodowska and Łodyga-Chruścińska, 2014; Khan et al., 2012; Rana et al., 2012). These compounds are structurally related to the *N*-acylhydrazones, being a more rigid and restrict analog of the latter. Both the nitrogen atoms of the structure, the one within the ring and the other at the thiazole 2-position, can establish hydrogen bonds as acceptor with amino acid residues as well as the sulfur atom at the ring, which is a isostere from oxygen atom present in carbonyl groups. The 4-phenyl ring car be an important point for hydrophobic interactions, such as observed by de Moraes Gomes et al. in their studies with 1,3-thiazoles as potential trypanocidal agents (de Moraes Gomes et al., 2016). The similarity of these groups with those present in peptide substrate of several enzymes could explain the set of different biological activity observed to 2-amiothiazole derivatives.

How far we have searched, however, there are few reports in the scientific literature about such compounds being exploited against parasites or helminths. Rajmane and Ubale, for instance, demonstrated that thiazole Schiff Bases derived from 4-(2'-halophenyl)-2-aminothiazoles exhibited nematocidal activity at very low concentrations against the plant parasite *Meloidogyne javanic*a as well as molluscicidal activity against the freshwater helminth vector snail *Lymnea auricularia* (Rajmane et al., 2013).

In this work, seventeen 4-(4-Substituted phenyl)-*N*-(4-substituted benzylidene)thiazole-2-amines were synthesized, characterized and tested *in vitro* on *S. mansoni* adult worms. Compounds were next tested on toxicity and further studied in mice harboring a chronic *S. mansoni* infection. Finally, *in silico* studies were also performed to predict potential macromolecular targets, as well as to foresee the oral absorption behavior of the best compound.

2. Material and methods

2.1. Material

All synthetic reagents are commercially available and were purchased from Sigma-Aldrich/Merck company (São Paulo-SP/Brazil). Solvents were obtained from LabSynth (Diadema-SP/Brazil) and used without previous treatment. Three-week-old female Swiss mice were purchased from Laboratory Animals Anilab (São Paulo, Brazil). Roswell Park Memorial Institute (RPMI 1640) culture medium containing phenol red and L-glutamine, M199 medium, inactivated fetal bovine serum (FBS), penicillin G/streptomycin sulfate, and HEPES buffer were obtained from Vitrocell (Campinas, SP, Brazil). DMSO employed to prepare compound's solutions was obtained from Sigma-Aldrich (São Paulo- SP/Brazil). The NMR spectra were recorded in a Bruker Advance 300 operating at 300 MHz for ^{1}H and 75 MHz for ^{13}C analysis. Chemical shifts (δ) were measured from tetramethylsilane (TMS) as internal reference and are reported in ppm. Coupling constants (J) are reported in Hz, when applicable. Infrared data were acquired in an IR Affinity-1 Shimadzu spectrometer, as KBr pellets and considering the wavenumbers from 4000 to 400 cm^{-1}.

Freeware and web-based softwares were employed in the Target Fishing studies, Autodock v.1.5.6 was used to perform the molecular docking studies while the pharmacokinetics predictions were performed with ADMET Predictor™ and GastroPlus™ softwares, both provided by Simulations Plus, Inc., Lancaster, CA, USA.

2.2. Methods

2.2.1. Synthesis

4-(4-Substituted phenyl)-*N*-(4-substituted benzylidene)-1,3-thiazole-2-amines were synthesized following a two-step reactional pathway. First, the intermediate 4-Substituted phenyl-1,3-thiazole-2-amines were obtained through the classical methodology of Hantzsch and Weber approach (Hantzsch and Weber, 1887). The Schiff bases were obtained, then, from the reaction of the corresponding 4-Substituted phenyl-1,3-thiazole-2-amine with different aldehydes at equimolar ratio and employing piperidine as catalyst (Geronikaki et al., 2004). Liquid chromatography in silica gel (hexane: ethylacetate, 7:3) was employed to purify the final compounds.

Structural characterization was performed by melting point range determination, carbon and hydrogen nuclear magnetic resonance, infrared spectroscopy. Data can be found at Supplementary Material.

2.2.2. Animals and parasite maintenance

This study was approved by the Comissão de Ética no Uso de Animais (CEUA), from Universidade Guarulhos (protocol no. 31/2017, Brazil). The animal studies are reported in compliance with the "Animal research: reporting of *in vivo* experiments" (ARRIVE) guidelines. Three-week-old female Swiss mice were purchased from Laboratory Animals Anilab (São Paulo, Brazil). They were housed in individually vented caging systems in groups of five mice per cage. Mice were kept under a 12-h light/12-h dark environment cycle and maintained at uniform temperature and humidity, with food and water available *ad libitum* (Lago et al., 2019). Mice were infected with *S. mansoni* (BH strain) by subcutaneous injection of ~80 cercariae. Cercariae were harvested from infected intermediate host snails *Biomphalaria glabrata* by exposure to light for 3 h, following standard procedures of our laboratory (Guimarães et al., 2015; Silva et al., 2017).

2.2.3. In vitro antischistosomal assay

Adult schistosomes were harvested from the hepatic portal veins and mesenteric veins of infected mice (7 weeks post-infection) and *in vitro* antischistosomal assay was performed as previously described (De Castro et al., 2015; Mafud et al., 2016). Briefly, parasites were placed in RPMI 1640 culture medium supplemented with 10% fetal bovine serum containing 100 IU/ml, penicillin and 100 μg/ml streptomycin at 37°C and 5% CO_2. All compounds were dissolved in DMSO and were initially tested at 100 μM in triplicate on adult *S. mansoni*. The compounds that produced an effect superior to 80% after 24 h post-exposure were considered as hits and underwent determination of their half-maximum lethal concentrations, LC_{50}, using 1:2 serial dilutions from 3.12 to 100 μM. Each concentration was tested in triplicate and the entire assay was repeated at least three times. Parasites were also incubated in the presence of the highest DMSO concentration (0.5%) as a negative control. LC_{50} value of praziquantel, used a positive control, was determined using 1:2 serial dilutions from 0.15 to 2.5 μM. The LC_{50} for active compounds were calculated with GraphPad Prism software using sigmoid dose-response curves and the 95% confidence intervals.

2.2.4. Cytotoxicity assay

The determination of cytotoxicity was performed with Vero cells (ATCC CCL-81; Manassas, VA) according to a previously reported procedure (de Brito et al., 2017). Briefly, cells were seeded in 96-well microtiter plates at a density of 5×10^4 cells/mL in DMEM medium with 10% fetal bovine serum and L-glutamine (2 mM). Compounds serially diluted 2-fold ranging from 15.62 to 500 μM in test medium were added. The plates were incubated at 37°C at an atmosphere of 5% CO_2. After 72 h, 3-(4,5-dimethylthiazol-2-yl)-2,5-diphenyltetrazolium bromide (MTT) was added and incubation was continued for another 3 h. The plate was then read using an Epoch™ 2 Microplate Spectrophotometer (BioTek) at 595 nm. Values were expressed as percentage of the control. Experiments were performed at least three times and IC_{50}

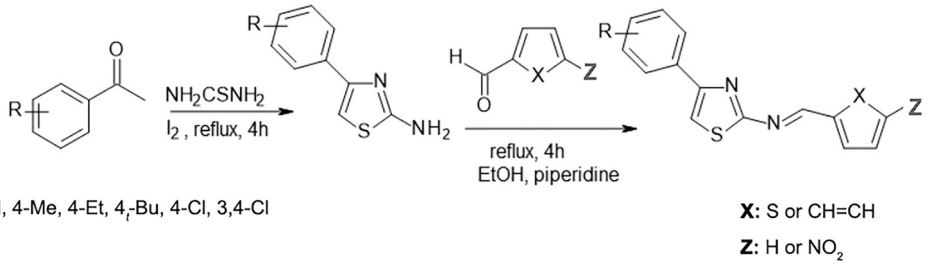

Fig. 1. Synthetic route of the compounds.

values calculated as averages. The selectivity indices (SI) of tested compounds were calculated by dividing CC_{50} values obtained on Vero cells with LC_{50} values determined on adult schistosomes (Rodrigues et al., 2018).

2.2.5. *In vivo* studies

In vivo antischistosomal assay was performed in a mouse model of schistosomiasis according to the operating procedures for experimental chemotherapy for antischistosomal drug (Lago et al., 2019). Groups of five infected mice characterized by a chronic schistosome infection (49 days post-infection) were treated orally with the test drug using single oral doses of 400 mg of compound per kg body weight. Five untreated mice served as controls. Two weeks post treatment, animals were euthanized with CO_2, dissected, and worms were sexed and counted (De Lima et al., 2018). Assessment of therapeutic efficacy was also based on the technique of quantitative and qualitative oograms using a fragment (10 mm) of the ascending colon, as well as the Kato-Katz method for quantitative feces examination. The compound-treated group and control group were compared using a parametric Dunnett's multiple-comparison test, where statistical significance was set to $P < 0.05$ in GraphPad Prism software (de Moraes et al., 2014). The animals were randomly assigned to the experimental groups, and pharmacological treatments were counterbalanced randomly as well. The animals were also euthanized in a random manner inside a group (Mengarda et al., 2020).

2.2.6. *Molecular modeling and in silico absorption studies*

Target fishing studies were performed employing a combination of GaussView 5.0, Gaussian 09W (Frisch et al., 2016), Pharmmapper Webserver (Liu et al., 2010) softwares and the Basic Local Alignment Search Tool, BLAST (Altschul et al., 1990).

Compounds were sketched in GaussView 5.0 and the tridimensional geometries optimized using PM6 semi-empirical force field. Following the structural optimization, energy optimization was performed by *ab initio* approach, employing method HF/6.31G* and ChelpG charges calculation. The files containing the geometric coordinates of the atoms and their ChelpG charges were, then, used as mol2 input in the Pharmmapper Web-based. This software was adjusted to search for all potential macromolecular targets (humans and not humans), and to perform 300 conformers generation.

A set of 100 results for each compound was retrieved from Pharmmapper and analyzed by their Z'Score, Fit Score and Normalized Fit Score values. The results of each compound were also compared to select only targets common to all seven analogues and, with the selected targets, a BLAST search was done to find similar proteins expressed by *Schistosomatidae* family, with special attention to those expressed by *S. mansoni*. Seven homolog proteins from *S. mansoni* proteome were selected as the best regarding the percentage of identity with the orthologue protein (more than 40%) and the statistics of the alignment, such as the E-value (lower than 10^{-50}) and Max-Score.

Docking studies were performed employing Autodock v. 1.5.6 free software and the structures of the known crystallized S. mansoni proteins, the Carbonic Anhydrase (PDB ID: 6QQM, resolution: 1.75 Å) and *S. mansoni* Arginase (PDB ID:4Q3Q, resolution: 2.00 Å). The proteins were prepared by adding the missing hydrogen atoms, removing all water molecules, setting the atom types to AD4 force field and by removing all non-essential ligands. Co-crystalized ligands were used as reference to the redocking studies and to the comparative analysis performed with GPQF-108. In the case of Carbonic Anhydrase, the known inhibitor ethoxzolamide (ETZ) was employed to this comparative analysis instead of glycerol, the co-crystalized ligand found in 6QQM model.

All ligands were prepared by setting the atom types, adding missing hydrogens, geometric optimization followed by energy minimization and had their Geisteiger charges calculated (Gaussian 09W software). Boron parameters were added to the AD4 parameter file (.dat). The specific parameter data is provided at Supplementary Material. Grid boxes of 50 × 50 × 50 Å, with centers at the zinc metal atom of carbonic anhydrase (X:-43.963; Y: 19.849; Z:-35.532) and in the center of the catalytic site of the Arginase 1, Chain A (X: -42.019; Y: -18.985; Z: 49.527) were employed as reference to the ligand docking simulation. Calculated energies of binding were used in the comparative analysis with GPQF-108.

Absorption predictions were performed with the ADMET Predictor™ software version 9.5 (Simulations Plus, Lancaster, CA, USA) using mol file of GPQF-108 employed as input. GastroPlus™ software 9.6 (Simulations Plus, Lancaster, CA, USA) was also used to predict the pharmacokinetic (PK) profile of the compound.

3. Results and discussions

3.1. *Synthesis*

Seventeen compounds were obtained through a fast and simple synthetic pathway (Fig. 1) but with low to moderate yields (Table 1).

The low obtained yields were probably related to the low nucleophilic power of the amino group of the 4-substituted-phenyl-1,3-thiazole-2-amine since, for all compounds, a certain amount of this starting material was observed by the end of the reactions. Liquid chromatography was, then, performed to purify the final Schiff bases.

Derivatives of the 5-nitrothiophene carboxaldehyde exhibited the lower yields values since the chromatography of nitro compounds is recognizable difficult due to their high affinity for silica gel. The same was true for the 4-nitrobenzaldehyde derivatives as well as better yields were obtained for the non-nitrated ones.

Compounds were structurally characterized by infrared spectroscopy, hydrogen and carbon nuclear magnetic resonance (^{1}H- and ^{13}C-NMR). Purities were accessed by a combination of melting point ranges (up to 4 °C) and ^{1}H-NMR spectra analysis, by considering the absence of signals other than the expected ones.

Results also prove the preferential synthesis of the *E* isomers, when regarding the azomethine double bond, since the NH signal appeared at 10 to 12 ppm, as well as no duplicated signal, suggesting the presence of the *Z* isomer, was observed. GPQF-102 and GPQF-118, conversely, presented duplicated signals, but in intensities coherent with the prevalence of the *E* isomers.

Table 1
Schiff bases of 4-substituted-phenyl-1,3-thiazole-2-amines.

General Structure	Ar/Het	GPQF	R_1	Yield* (%)	Melting Point °C
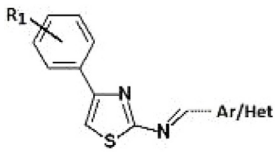	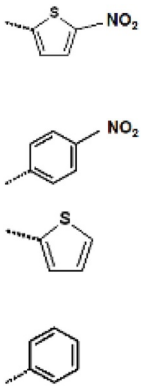	108	H	9	150–154
		109	4-Me	12	152–156
		110	4-Et	10	137–141
		113	4-$_{Tert}$Bu	10	164–168
		115	4-Cl	4	115–119
		101	4-Me	19	152–155
		102	4-Et	9	127–130
		107	H	22	149–153
		116	4-Cl	17	155–157
		117	4-Me	55	116–118
		118	3,4-Cl	19	88–91
		122	H	54	94–98
		123	4-Et	22	103–106
		124	4-Cl	52	115–118
		132	4-Et	30	92–94
		133	4-Me	23	133–136
		134	4-Cl	51	129–132

* Yields obtained after liquid chromatography purification.

3.2. In vitro assays

Once characterized, the seventeen compounds were evaluated to their potential to inhibit the *S. mansoni* adult worms through *in vitro* screening as well as had their cytotoxicity toward VERO cells assessed (Table 2). Selectivity indexes were calculated as the proportion between the CL_{50} and IC_{50} values.

GPQF-108 was notably the most interesting analog with an IC_{50} value of 29.44 μM associated to a CL_{50} value of 179.44, which corresponds to a selectivity index of approximately 6.1. GPQF-110 and 113 presented a very similar biological behavior, being the second most active compounds of the series. GPQF-115 was the third in potency (IC_{50}: 51.31 μM) against adult worms but showed a selectivity index (3.72) lower than GPQF-109, which was less active, but seems to be more selective (IC_{50} value of 60.17 μM but SI of 5.11). All compounds were considerably less active than PZQ when tested against schistosomes *in vitro*.

Noteworthy is the fact that only the derivatives of 5-nitro-2-thiophenecarboxaldehyde were active. The nitro group seems to be explicitly involved in the mechanism of action, since the corresponding derivatives of thiophenecarboxaldehyde did not show any significant activity.

Table 2
In vitro activities and selectivity indexes

GPQF	IC_{50} (μM) [*]	CL_{50} (μM) [*]	SI
108	29.44 [20.04–37.16]	179.44 [148.93–202.47]	6.10
109	60.17 [52.12–74.06]	307.54 [273.91–334.41]	5.11
110	33.96 [26.77–45.05]	187.15 [150.14–223.27]	5.51
113	38.02 [32.49–46.01]	205.68 [178.76–249.89]	5.41
115	51.31 [44.61–62.88]	191.03 [158.09–227.98]	3.72
101	>100	ND	ND
102	>100	ND	ND
107	>100	ND	ND
116	>100	>100	ND
117	>100	>100	ND
118	>100	>100	ND
122	>100	>100	ND
123	>100	>100	ND
124	>100	>100	ND
132	>100	>100	ND
133	>100	>100	ND
134	>100	>100	ND
PZQ	1.08 [0.71–1.46]	>100	>50

ND: Not determined; [*]: Confidence Interval. PZQ: praziquantel (positive control).

One could conclude that the most common mechanism of action of such compounds, the nitro reduction by unspecific nitroreductases, would be the most probable explanation for the observed anti-schistosomal activity (Race et al., 2005). This hypothesis, however, is uncertain since all the 5-nitrobenzaldehyde analogs tested were also inactive against the adult worms. Moreover, nitro reduction is a mechanism associated with some toxicity toward mammalian cells, which was not observed in the VERO cytotoxicity assays, even with the active compounds, which presented CL_{50} values above 150 μM.

The nitro group alone, thus, is not responsible for the total activity of these compounds. It seems it must be bonded to a heterocyclic aromatic ring. The need for a heteroatom in the ring can point to some electronic contribution of this atom. Studies with a larger series of active compound could elucidate this point.

3.3. In vivo assays

Due to its significant performance in this first *in vitro* assay, GPQF-108 was elected to be studied to its potential antischistosomal activity in a mouse model. Worm burden, egg production and hepato- and splenomegaly were examined after a single oral dose of 400 mg/kg, administered 42 days after infection to mice harboring adult *S. mansoni* (chronic infection). Fig. 2 shows that treatment with GPQF-108 resulted in a significant reduction of ~54% ($P < 0.01$) for the total worm

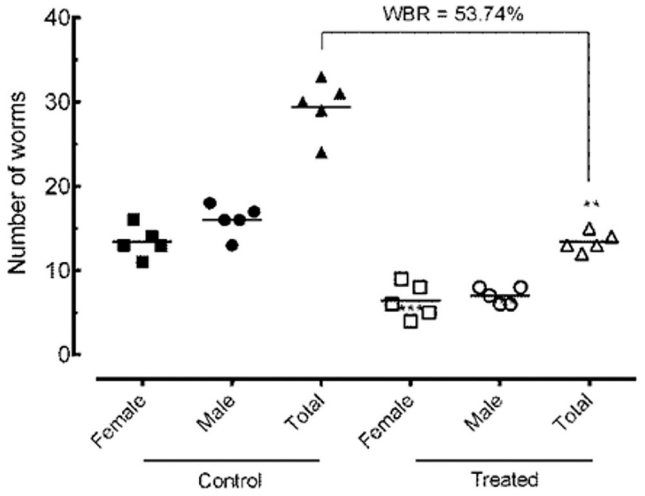

Fig. 2. Effect of GPQF-108 on the parasite burden of mice infected with *S. mansoni*.

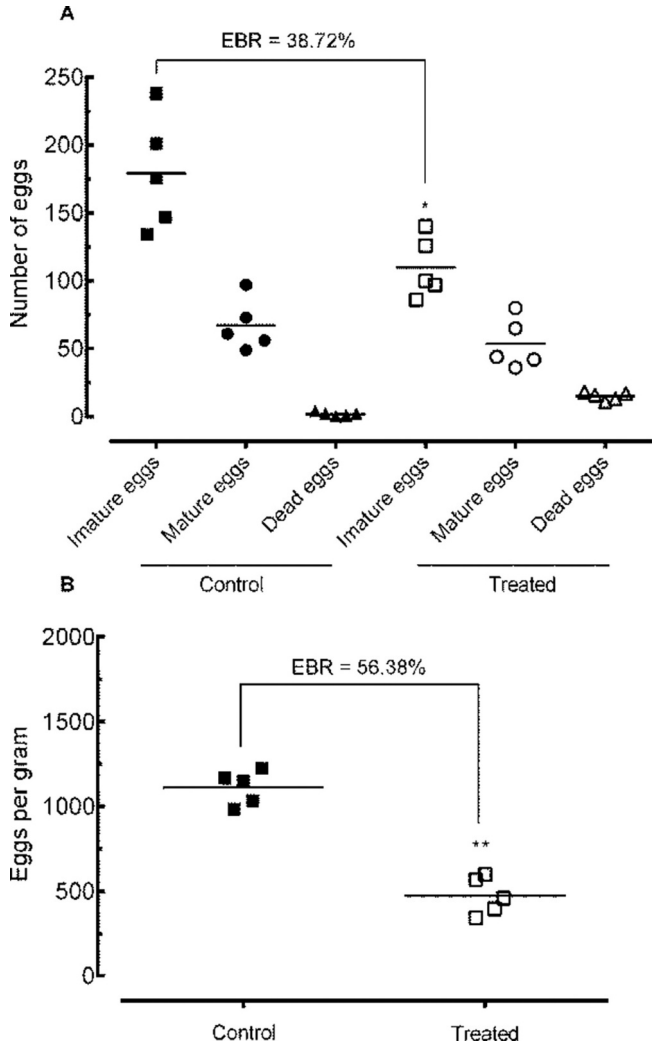

Fig. 3. Effect of GPQF-108 on the egg burden of mice infected with *S. mansoni*.

burden.

The sexually mature male and female worms pair up and the female produces hundreds to thousands of eggs a day, half of which become trapped in tissues while the other eggs are eliminated by the feces. With respect to egg burden, samples of intestinal tissue were used to study the percent egg developmental stages (oogram), including the number of egg in fecal samples by the Kato-Katz method. As shown in Fig. 2, a single oral dose of GPQF-108 led to a reduction of 38.72% ($P < 0.05$) in the number of immature eggs (Fig. 3A), whereas analysis in fecal samples revealed a reduction of 56.38% ($P < 0.01$) of eggs (Fig. 3B). This finding could be attributed to a reduction in the worm burden as a result of treatment with GPQF-108 and/or inhibition of oviposition by adult helminths.

Points represent data from individual mice. Horizontal bars represent median values. ** $P < 0.01$ compared with untreated groups. Squares: females, Circles: males, Triangles: Total, Filled symbols: control, Empty symbols: treated. WBR: Worm burden reduction.

A: Egg development stages (oogram). B: stool egg load. Points represent data from individual mice. Horizontal bars represent median values. ** $P < 0.05$, ** $P < 0.01$ compared with untreated groups. In A = Squares: Immature eggs, Circles: Mature eggs, Triangles: Dead eggs, Filled symbols: control, Empty symbols: treated. In B = Squares: eggs per gram. Filled and Empty symbols correspond to control and treated group, respectively. EBR: Egg burden reduction.

The eggs are crucial for the maintenance of the schistosome life cycle and disease transmission and are further responsible for

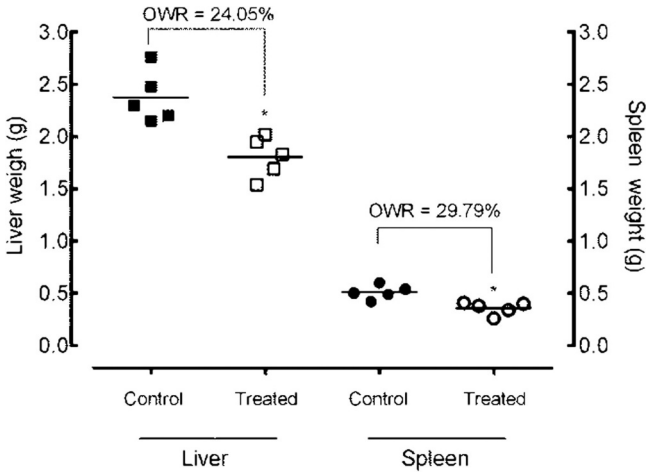

Fig. 4. Effect of GPQF- 108 on the liver and spleen pathology of mice infected with *S. mansoni*.

manifested human pathology. The protective effect of GPQF-108 was also found to lead to a reduction of hepato- and splenomegaly, as measured by weight, compared to the control infected mice. In more details, liver and spleen weights were significantly decreased by 24.05% ($P < 0.05$) and 29.79% ($P < 0.05$), respectively. This result could be attributed to a reduction in the worm burden and oviposition (Fig. 4).

Horizontal bars represent median values. *$P < 0.05$, compared with untreated groups. Squares: liver weigh, Circles: spleen weigh, Filled symbols: control, Empty symbols: treated. OWR: Organ weight reduction.

In tandem, oral treatment with GPQF-108 in mice harboring chronic infections significantly reduced worm burden, egg production, and hepato- and splenomegaly. Comparatively, the antischistosomal effect of GPQF-108 is weaker than praziquantel, which is known to reduce ~90% of the worm burden. (Roquini et al., 2019; Guerra et al., 2019) Despite of not achieving the same potency presented by Praziquantel and other known drugs, it is important to highlight that GPQF-108 is herein considered as a starting point to be explored to find new antischistosomal drugs with a scaffold different from the standard drug and, for this reason, a good alternative in case of resistance emergence.

3.4. Target fishing studies

In order to propose possible macromolecular targets through which the active 5-nitrothiophene derivatives could be acting (besides the nitro reduction known mechanism), a target fishing study was performed employing the Pharmmapper software. One-hundred targets were retrieved to each analogue (active and inactive ones) and 12 macromolecules were selected to further studies since they were common to all active 5-nitrothiophene derivatives (Table 1, Supplementary Material).

Targets are listed following the best Z'scores obtained to the best compound, GPQF-108. None of the found targets was exhibited exclusively for GPQF-108, since this is a congeneric series and, as such, the compounds present several structural similarities which could guarantee the presence of the pharmacophores in more than one analogue. Differences in activity should result, thus, from other characteristics such as, the ability to be transported through the worm tegument or to achieve the target.

Despite good statistical data, none of the target fishing resulting macromolecules corresponds to crystals of proteins expressed by worms from *Schistosomatidae* family. For this reason, a BLAST (Basic Local Alignment Search Tool, National Center for Biotechnology Information) search was performed to find homologous proteins in the *S. mansoni*

Table 3
Results from target fishing after BLAST analysis.

Target PDB	Blast alignment results				
	S. mansoni Ortholog Proteins	Identity (%)	E-Value	Max Score	State of Art
1KE5	Serine/Threonine Kinase	60.54	$9e^{-129}$	374	known
3CP9	Tyrosine kinase	40.13	$6e^{-63}$	211	known
1BNV	Carbonic Anhydrase	40.23	$1e^{-61}$	196	known
1D3V	Chain A Arginase-1	41.72	$3e^{-82}$	255	known
1VZC	Uncharacterized Protein Sm_200410	42.72	$4e^{-81}$	250	known
2CNG	Tyrosine Phosphatase, non-receptor type nt1	45.05	$1e^{-83}$	265	putative

available proteome (Altschul et al., 1990).

Six *S. mansoni* proteins exhibited suitable structural correspondence to the targets obtained with Pharmmapper. They are listed in Table 3 together with the statistical analyses which support their significance.

Five out of the six best BLAST results are known proteins of the *S. mansoni*, while one of them is a putative protein. Kinase families were pointed out as potential targets.

Serine/Threonine Kinases and Tyrosine Kinases are families of kinases widely distributed among eukaryotes. It has already been reported the expression of different serine/threonine and tyrosine kinases by *S. mansoni*, such as Ctk, Src, Fyn and Syk as well as members of the Fes family. These proteins are found at worm subtegument, parenchyma, gastrodermis, ovary and testicles (Bahia et al., 2007; Grevelding et al., 2018; Kapp et al., 2004, 2001). Known inhibitors of these kinases such as Herbimycin and Imatinib lead to oogenesis and spermatogenesis alterations when assayed against *S. mansoni* adult worms (Knobloch et al., 2006; Manley et al., 2002). Both studies, yet, demonstrated significant morphological alterations and decrease in egg production, the same effect obtained with the exposition to GPQF-108. Since these are broad classes of proteins, further studies must be conducted to elucidate if they could be genuine targets of this Schiff base.

Other interesting macromolecular target would be the "Uncharacterized Protein Sm_200410", which corresponds to the Thymidylate synthase *S. mansoni* orthologue enzyme (Kouni, 2017). Despite presenting a fundamental role in eukaryote nucleotides synthesis, this protein has never been explored as a macromolecular target for schistosomiasis. The effect of its inhibition probably would be the worm death, but selectivity toward helminth enzyme would be a challenge. Nevertheless, several thymidylate synthase drugs are available in the market and selectivity against pathogens are a recognizable possibility.

Arginase-1, *Sm*ARG, is expressed at all life forms of the helminth and seems to present an important role in host immune response evasion. This enzyme is also present in other pathogens, such as *Leishmania sp, Helicobacter pylori* as well as in cancer cells and had its role in lowering host immune response well defined and could provide a macromolecular target to be explored (Gaur et al., 2007; Hai et al., 2014; Zabaleta et al., 2004).

Regarding the Tyrosine Phosphatase non-receptor type nt1, although it had been extensively studied in several eukaryote, little is known about their role to the *S. mansoni* helminth (Protasio et al., 2012).

Recently elucidated by crystallography, the zinc-dependent metalloenzyme *S. mansoni* Carbonic Anhydrase could constitute an interesting target to new therapeutics (Da'dara et al., 2019). Responsible for catalyzing the reversible conversion of carbon dioxide and water into bicarbonate ion and ionic hydrogen, this enzyme is found on the tegument surface of the *S. mansoni* and seems to present a role in the regulation of the acid-basic homeostasis at the parasite surface as well as in the osmotic balance. Its inhibition could promote a lack of osmotic balance (Castro-Borges et al., 2011). Interesting, this same target was recently identified, by our group, as a potential target to a vanillin-related *N*-acylhydrazone which presents structural similarities with the Schiff bases herein reported (Rando et al., 2019).

Two of the pointed *S. mansoni* targets, the Carbonic Anhydrase and the Arginase-1, had their crystal structure elucidated by X-Ray Crystallography and, for this reason, molecular docking studies with these two targets were performed employing Autodock 4 software.

Fig. 5A shows the simulated docking of the ethoxzolamide (ETZ) within the *S. mansoni* Carbonic Anhydrase (SmCA). This compound was demonstrated to be a good, but not selective, inhibitor of the SmCA by Da'dara et al. (Da'dara et al., 2019) and, in fact, its simulation at the enzyme's active site resulted in the best pose exhibiting an energy of binding of -5.36 kcal/mol. It also showed a binding mode very similar to those observed to this same compound when co-crystalized with the human enzyme (hCAII, PDB ID: 3CAJ). Hydrogen bonds with the Thr231 and Thr232 are observed as well as a pi-staking interaction with thehis177 imidazole ring. The ETZ was employed here as the known inhibitor of the SmCA since, the co-crystalized compound of the used geometric model was the glycerol, a promiscuous ligand and not a good alternative to serve as reference to SmCA binding mode.

Under the same simulation conditions, GPQF-108 adjusted to the SmCA catalytic site quite similarly to the observed with ETZ (Fig. 5B). An energy of binding of -4.8 kcal/mol was calculated, a little bit higher than the ETZ, but the compound established interactions with Gln115 residue through the nitrogen from the thiazole ring. Hydrogen bond is also present between the nitro group and the His119. This result could explain, in part, the nitro group importance to the observed activity. This group approaches the Zn^{2+} metal cofactor, fundamental to the SmCA activity, and established interactions within the cavity through its oxygen atoms. This may be the reason why non-nitrated analogs did not exhibited activity.

It is noteworthy the similar fitting of both ligands within in the actives site of SmCA (Fig. 5C).

Fig. 5D, in turn, shows the results obtained to the docking simulations with the Arginase-1, chain A, enzyme and the known and co-crystallized ligand 2(S)-Amino-6-Boronohexanoic Acid (ABH). This compound achieved an energy of binding of –8.98 kcal/mol and exhibited the same interactions observed in the crystal structure (4Q3Q). These involves a series of hydrogen bond interacts mainly established with the Gly157, Asp158, Ile159, Asp154, Asp264 and even with the two manganese ions (Mn^{2+}) present as cofactors of this enzyme.

The simulations with GPQF-108 showed that it docked in a similar position (Fig. 5E) and exhibited an even better calculated energy of binding, of -9.24 kcal/mol. It established interactions with Asp158, Asp264, His131and Thr276 through its nitro group and a pi-stacking interaction with the His156. Again, the nitro group approaches de ions Mn^{2+} from the catalytic site in distances compatible with ion-dipole interactions (1.63 and 1.65 Å from the Mn^{2+} 1 and 2 in Fig. 5E).

Legend: Carbon, nitrogen, oxygen, hydrogen and sulfur atoms are represented in gray, blue, red, white and yellow tubes. Carbon atoms of the ligands are represented in magenta for "known inhibitors" and in green for GPQF-108. Thin tubes represent protein atoms, while bold tubes represent the ligands. Three-letter amino acid code was employed.

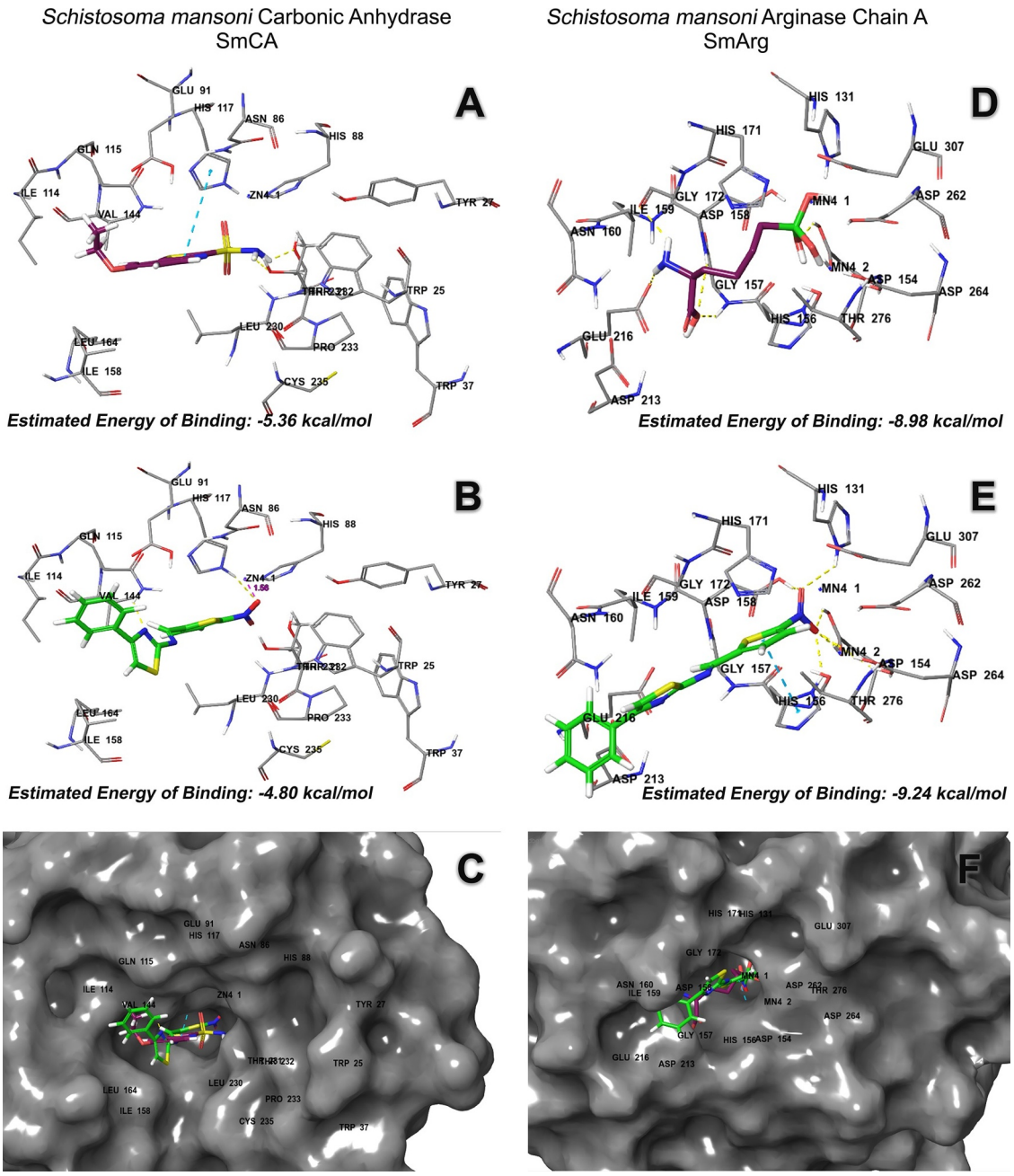

Fig. 5. Docking simulation studies with GPQF-108 and the *Schistosome mansoni* enzymes SmCA and SmArg.

Once more, both compounds exhibited similar fitting within the active cavity of the SmArg enzyme (Fig. 5F).

These results reinforce the potential of the GPQF-108, and maybe its analogues, of act through inhibition of these enzymes. Only experimental assays; however, could confirm the real inhibitory potential of the GPQF-108 and its analogs toward these *S. mansoni* targets.

3.5. *In silico* absorption and bioavailability studies

Finally, *in silico* studies were performed to predict key physical-chemical and biopharmaceutical properties of GPQF-108 as well as its oral bioavailability. Some properties, such as pKa, LogP, $LogD_{7.4}$, Water Diffusion Coefficient, Jejune Effective Permeability and Water solubility were calculated using ADMET Predictor™ software. Results pointed out the dominance of the basic amino groups in the structure and the expected inability of ionization of it, through identical LogP and $LogD_{7.4}$ values (Table 4).

Table 4
Absorption prediction parameters

Property	Predicted values
pKa (S + Basic_pKa)[a,*]	1.71–2.27
LogP	3.191
$LogD_{7.4}$	3.191
Molecular Weigh (g/mol)	315.37
DiffCoef[b]	0.804
S + Peff[c,*]	4.582
S + SW (mg/mL)[d,*]	8.130×10^{-5}

[a] pKa predicted ionization coefficient
[b] Water Diffusion Coefficient (cm/s x 10^{-5})
[c] Jejune Effective Permeability (cm^2/s x 10^{-4})
[d] Water Solubility (mg/mL)
[*] S+ = Simulations Plus algorithm

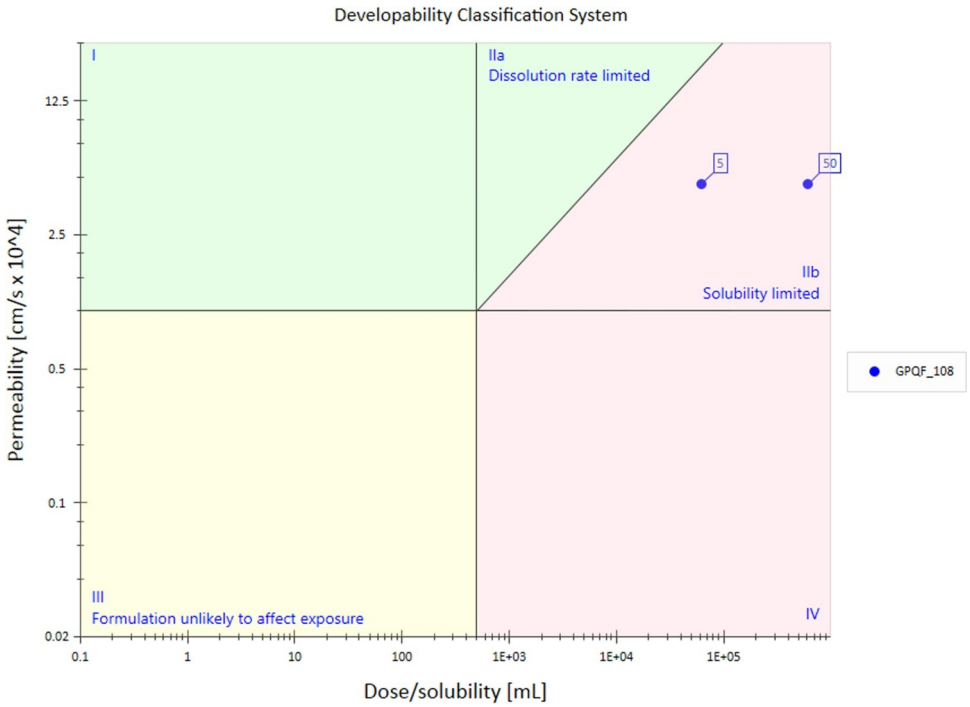

Fig. 6. – BCS/DCS classification of GPQF-108.

Based on these values (Table 4), the BCS/DCS Explorer tool in ADMET Predictor™ was used to predict the classification according to the Biopharmaceutical Classification System (BCS) (Amidon et al., 1995) and the Developability Classification System (DCS) (Butler and Dressman, 2010) of the compound.

The BCS classifies the drugs into four classes according to the aqueous solubility in physiology pH range and intestinal permeability: class I (high solubility and high permeability), class II (low solubility and high permeability), class III (high solubility and low permeability) and class IV (low solubility and low permeability). The volume of 250 mL of buffer solutions is used for BCS solubility classification. The DCS proposes changing the volume to 500 mL and the addition of two subclasses for BCS class II compounds: class IIa and class IIb. The BCS/DCS classification of GPQF-108 obtained using ADMET Predictor™ software is shown in Fig. 6.

According to the results pointed out in Table 4 the estimated (Fig. 4) BCS classification of GPQF-108 is class II (low solubility and high permeability) and the DCS classification is class IIb. This indicates that GPQF-108 could present absorption limited by its solubility. Moreover, class IIb compounds tend to have incomplete intestinal absorption (Butler and Dressman, 2010).

The parameters DiffCoef and S + SW corroborate the difficult water media diffusion of GPQF-108. Globular compounds are more suitable to diffuse in water media, but GPQF-108, as all other 4-(4-Substituted phenyl)-*N*-(4-substituted benzylidene)thiazole-2-amines, is planar due to its extended electronic conjugation.

ADMET Predictor™ has the Lipinski's Rule of 5 (Ruleof5) descriptor. This score indicates the number of potential oral absorption problems a compound would have. The predicted value for GPQF-108 was 0.000, which means that this compound appeared to be Rule of 5 compliant. Predictions of oral absorption with GastroPlus™ software, however, revealed that the lower the particle size, the higher its oral absorption and bioavailability (Table 2, Supplementary material). This compound presented low predicted bioavailability values, which can be improved by formulation strategies to enhance its solubility.

MaxRTD (mg/Kg/day), the maximum recommended therapeutic dose administered as oral dose, estimated by ADMET Predictor™ was < 3.16. Based on this result, a daily oral dose of 2.5 mg/Kg, for an adult man with 70 Kg, was used in GastroPlus™ to predict PK values. Other calculated parameters in GastroPlus™ include the expected half-life [T1/2, h)] and plasma clearance (L/h) of GPQF-108. It could be expected a 12.13 h as $T_{1/2}$ and a clearance of 3.04 L/h for GPQF-108, which are values compatible with a once a day dose. Despite of the intestinal solubility problems, the herein predicted pharmacokinetic aspects indicate the druggability of GPQF-108.

In conclusion, GPQF-108 exhibited a promising activity/selectivity profile, but it was still deficient when compared to the standard drug, the praziquantel. This compound, however, posed as a good hit to be optimized in the search for new antischistosomal drugs. By means of rational chemical modifications, it would be possible to improve both activity and the absorption aspects which, as presented, does not need much effort to accomplish. If these compounds keep showing suitable biological profile, extensive in vivo and off-target activities should be performed to guarantee the efficacy and safety.

Chemical diversity is exactly what is desired when looking for alternative drugs to a previous one which is under the risk of resistance emergence. Moreover, the Schiff bases of 4-Phenyl-2-aminothiazoles presents a completely unexplored chemical structure, mainly regarding activity against the *Schistosomatidae* family, which can be obtained through a fast and economic synthetic pathway, an aspect to be considered in the search for drugs to treat neglected diseases.

The results herein reported open a new chemical field to be explored in the search for alternatives drugs to treat *Schistosomiasis*.

Funding sources

This work was supported by São Paulo Research Foundation (FAPESP, Brazil, grant 2013/01875-0) and Brazilian National Council for Scientific and Technological Development (CNPq, grant 408581/2018-2). TFAP, ACM and MPS were supported by a fellowship from the Brazilian Federal Agency for Support and Evaluation of Graduate Education (CAPES). J.M. also received established investigator fellowship from CNPq.

CRediT authorship contribution statement

Carina R. Amorim: Investigation, Methodology, Data curation. **Thais F.A. Pavani:** Methodology, Data curation, Writing - original draft, Writing - review & editing. **Andrey F.S. Lopes:** Investigation, Methodology, Data curation, Software. **Marcelo D. Duque:** Conceptualization, Methodology, Data curation, Software, Writing - original draft. **Ana C.A. Mengarda:** Investigation, Methodology, Data curation. **Marcos P. Silva:** Investigation, Methodology, Data curation. **Josué de Moraes:** Conceptualization, Writing - original draft, Funding acquisition. **Daniela G.G. Rando:** Supervision, Conceptualization, Validation, Project administration, Writing - review & editing, Funding acquisition.

Declaration of Competing Interest

The authors of this study declare no conflicts of interest.

Acknowledgment

We thank all of J. de Moraes's laboratory for help in maintaining the *S. mansoni* life cycle. We also thank Daniel B. Roquini and Tais C. Silva for support during *in vivo* studies.

Portions of these results were generated by ADMET Predictor™ and GastroPlus™ software provided by Simulations Plus, Inc., Lancaster, CA, USA.

Supplementary materials

Supplementary material associated with this article can be found, in the online version, at doi:10.1016/j.ejps.2020.105371.

References

Altschul, S.F., Gish, W., Miller, W., Myers, E.W., Lipman, D.J., 1990. Basic local alignment search tool. J. Mol. Biol. 215, 403–410. https://doi.org/10.1016/S0022-2836(05)80360-2.

Amidon, G.L., Lennernäs, H., Shah, V.P., Crison, J.R., 1995. A theoretical basis for a biopharmaceutic drug classification: the correlation of in vitro drug product dissolution and in vivo bioavailability. Pharm. Res. An Off. J. Am. Assoc. Pharm. Sci. https://doi.org/10.1023/A:1016212804288.

Bahia, D., Mortara, R.A., Kusel, J.R., Andrade, L.F., Ludolf, F., Kuser, P.R., Avelar, L., Trolet, J., Dissous, C., Pierce, R.J., Oliveira, G., 2007. Schistosoma mansoni: expression of Fes-like tyrosine kinase SmFes in the tegument and terebratorium suggests its involvement in host penetration. Exp. Parasitol. 116, 225–232. https://doi.org/10.1016/j.exppara.2007.01.009.

Brodowska, K., Łodyga-Chruścińska, E., 2014. Schiff bases - interesting range of applications in various fields of science. Chemik 68, 129–134. https://doi.org/10.1002/chin.201511346.

Butler, J.M., Dressman, J.B., 2010. The developability classification system: application of biopharmaceutics concepts to formulation development. J. Pharm. Sci. 99, 4940–4954. https://doi.org/10.1002/jps.

Castro-Borges, W., Dowle, A., Curwen, R.S., Thomas-Oates, J., Wilson, R.A., 2011. Enzymatic shaving of the tegument surface of live schistosomes for proteomic analysis: a rational approach to select vaccine candidates. PLoS Negl. Trop. Dis. 5. https://doi.org/10.1371/journal.pntd.0000993.

Cioli, D., Pica-Mattoccia, L., Basso, A., Guidi, A., 2014. Schistosomiasis control: praziquantel forever? Mol. Biochem. Parasitol. 195, 23–29. https://doi.org/10.1016/j.molbiopara.2014.06.002.

Da'dara, A.A., Angeli, A., Ferraroni, M., Supuran, C.T., Skelly, P.J., 2019. Crystal structure and chemical inhibition of essential schistosome host-interactive virulence factor carbonic anhydrase SmCA. Commun. Biol. 2, 1–11. https://doi.org/10.1038/s42003-019-0578-0.

de Brito, M.R.M., Peláez, W.J., Faillace, M.S., Militão, G.C.G., Almeida, J.R.G.S., Argüello, G.A., Szakonyi, Z., Fülöp, F., Salvadori, M.C., Teixeira, F.S., Freitas, R.M., Pinto, P.L.S., Mengarda, A.C., Silva, M.P.N., Da Silva Filho, A.A., de Moraes, J., 2017. Cyclohexene-fused 1,3-oxazines with selective antibacterial and antiparasitic action and low cytotoxic effects. Toxicol. Vitr. 44, 273–279. https://doi.org/10.1016/j.tiv.2017.07.021.

De Castro, C.C.B., Costa, P.S., Laktin, G.T., De Carvalho, P.H.D., Geraldo, R.B., De Moraes, J., Pinto, P.L.S., Couri, M.R.C., Pinto, P.D.F., Da Silva Filho, A.A., 2015. Cardamonin, a schistosomicidal chalcone from Piper aduncum L. (Piperaceae) that inhibits Schistosoma mansoni ATP diphosphohydrolase. Phytomedicine 22, 921–928. https://doi.org/10.1016/j.phymed.2015.06.009.

De Lima, L.I., Py-Daniel, K.R., Guimarães, M.A., Muehlmann, L.A., Mafud, A.C., Mascarenhas, Y.P., Moraes, J.De, De Souza De Almeida Leite, J.R., Jiang, C.S., Azevedo, R.B., Figueiró Longo, J.P., 2018. Self-nanoemulsifying drug-delivery systems improve oral absorption and antischistosomal activity of epiisopiloturine. Nanomedicine 13, 689–702. https://doi.org/10.2217/nnm-2017-0308.

de Moraes Gomes, P.A.T., de Oliveira Barbosa, M., Farias Santiago, E., de Oliveira Cardoso, M.V., Capistrano Costa, N.T., Hernandes, M.Z., Moreira, D.R.M., da Silva, A.C., dos Santos, T.A.R., Pereira, V.R.A., Brayner dos Santosd, F.A., do Nascimento Pereira, G.A., Ferreira, R.S., Leite, A.C.L., 2016. New 1,3-thiazole derivatives and their biological and ultrastructural effects on Trypanosoma cruzi. Eur. J. Med. Chem. 121, 387–398. https://doi.org/10.1016/j.ejmech.2016.05.050.

de Moraes, J., de Oliveira, R.N., Costa, J.P., Junior, A.L.G., de Sousa, D.P., Freitas, R.M., Allegretti, S.M., Pinto, P.L.S., 2014. Phytol, a diterpene alcohol from chlorophyll, as a drug against neglected tropical disease Schistosomiasis mansoni. PLoS Negl. Trop. Dis. 8, 51. https://doi.org/10.1371/journal.pntd.0002617.

Fenwick, A., Webster, J.P., 2006. Schistosomiasis: challenges for control, treatment and drug resistance. Curr. Opin. Infect. Dis. 19, 577–582. https://doi.org/10.1097/01.qco.0000247591.13671.6a.

Gaur, U., Roberts, S.C., Dalvi, R.P., Corraliza, I., Ullman, B., Wilson, M.E., 2007. An effect of parasite-encoded arginase on the outcome of Murine Cutaneous Leishmaniasis. J. Immunol. 179, 8446–8453. https://doi.org/10.4049/jimmunol.179.12.8446.

Geronikaki, A.A., Dearden, J.C., Filimonov, D., Galaeva, I., Garibova, T.L., Gloriozova, T., Krajneva, V., Lagunin, A., Macaev, F.Z., Molodavkin, G., Poroikov, V.V., Pogrebnoi, S.I., Shepeli, F., Voronina, T.A., Tsitlakidou, M., Vlad, L., 2004. Design of new cognition enhancers: from computer prediction to synthesis and biological evaluation. J. Med. Chem. 47, 2870–2876. https://doi.org/10.1021/jm031086k.

Grevelding, C.G., Langner, S., Dissous, C., 2018. Kinases: molecular stage directors for schistosome development and differentiation. Trends Parasitol. 34, 246–260. https://doi.org/10.1016/j.pt.2017.12.001.

Gryseels, B., Mbaye, A., De Vlas, S.J., Stelma, F.F., Guissé, F., Van Lieshout, L., Faye, D., Diop, M., Ly, A., Tchuem-Tchuenté, L.A., Engels, D., Polman, K., 2001. Are poor responses to praziquantel for the treatment of Schistosoma mansoni infections in Senegal due to resistance? An overview of the evidence. Trop. Med. Int. Heal. 6, 864–873. https://doi.org/10.1046/j.1365-3156.2001.00811.x.

Guerra, R.A., Silva, M.P., Silva, T.C., Salvadori, M.C., Teixeira, F.S., De Oliveira, R.N., Rocha, J.A., Pinto, P.L.S., De Moraes, J., 2019. In vitro and in vivo studies of spironolactone as an antischistosomal drug capable of clinical repurposing. Antimicrob. Agents Chemother. 63, 1–11. https://doi.org/10.1128/AAC.01722-18.

Guimarães, M.A., de Oliveira, R.N., Véras, L.M.C., Lima, D.F., Campelo, Y.D.M., Campos, S.A., Kuckelhaus, S.A.S., Pinto, P.L.S., Eaton, P., Mafud, A.C., Mascarenhas, Y.P., Allegretti, S.M., de Moraes, J., Lolić, A., Verbić, T., Leite, J.R.S.A., 2015. Anthelmintic activity in vivo of epiisopiloturine against juvenile and adult worms of Schistosoma mansoni. PLoS Negl. Trop. Dis. 9, 1–19. https://doi.org/10.1371/journal.pntd.0003656.

Hai, Y., Edwards, J.E., Van Zandt, M.C., Hoffmann, K.F., Christianson, D.W., 2014. Crystal structure of Schistosoma mansoni arginase, a potential drug target for the treatment of schistosomiasis. Biochemistry 53, 4671–4684. https://doi.org/10.1021/bi5004519.

Hantzsch, A., Weber, J.E., 1887. Ueber verbindungen des thiasola (Pyridine der Thiophenreihe). Dtsch. Chem. Gesellschaft 20, 3118–3132. https://doi.org/10.1002/cber.188702002200.

Kapp, K., Knobloch, J., Schüßler, P., Sroka, S., Lammers, R., Kunz, W., Grevelding, C.G., 2004. The Schistosoma mansoni Src kinase TK3 is expressed in the gonads and likely involved in cytoskeletal organization. Mol. Biochem. Parasitol. 138, 171–182. https://doi.org/10.1016/j.molbiopara.2004.07.010.

Kapp, K., Schüßler, P., Kunz, W., Grevelding, C.G., 2001. Identification, isolation and characterization of a Fyn-like tyrosine kinase from Schistosoma mansoni. Parasitology 122, 317–327. https://doi.org/10.1017/S0031182001007430.

Khan, khalid mohammed, Ambreen, N., Karim, A., Saied, S., Amyn, A., Ahmed, A., Shahnaz Perveen, 2012. Schiff bases of thiazole as antibacterial and antifungal agents5, 651–656.

Knobloch, J., Kunz, W., Grevelding, C.G., 2006. Herbimycin A suppresses mitotic activity and egg production of female Schistosoma mansoni. Int. J. Parasitol. 36, 1261–1272. https://doi.org/10.1016/j.ijpara.2006.06.004.

Kouni, M.H., 2017. Pyrimidine metabolism in schistosomes: a comparison with other parasites and the search for potential chemotherapeutic targets. Comp. Biochem. Physiol. B Biochem. Mol. Biol. 213, 55–80. https://doi.org/10.1016/j.cbpb.2017.07.001.

Lago, E.M., Silva, M.P., Queiroz, T.G., Mazloum, S.F., Rodrigues, V.C., Carnaúba, P.U., Pinto, P.L., Rocha, J.A., Ferreira, L.L.G., Andricopulo, A.D., de Moraes, J., 2019. Phenotypic screening of nonsteroidal anti-inflammatory drugs identified mefenamic acid as a drug for the treatment of schistosomiasis. EBioMedicine 43, 370–379. https://doi.org/10.1016/j.ebiom.2019.04.029.

Lago, E.M., Xavier, R.P., Teixeira, T.R., Silva, L.M., Da Silva Filho, A.A., De Moraes, J., 2018. Antischistosomal agents: state of art and perspectives. Future Med. Chem. 10, 89–120. https://doi.org/10.4155/fmc-2017-0112.

Liu, X., Ouyang, S., Yu, B., Liu, Y., Huang, K., Gong, J., Zheng, S., Li, Z., Li, H., Jiang, H., 2010. PharmMapper server: a web server for potential drug target identification using pharmacophore mapping approach. Nucleic Acids Res. 38, 5–7. https://doi.org/10.1093/nar/gkq300.

M. J. Frisch, G. W. Trucks, H. B. Schlegel, G. E. Scuseria, M. A. Robb, J. R. Cheeseman, G. Scalmani, V. Barone, G. A. Petersson, H. Nakatsuji, X. Li, M. Caricato, A. Marenich, J. Bloino, B. G. Janesko, R. Gomperts, B. Mennucci, H. P. Hratchian, J. V. Ort, and D.J. F., 2016. Gaussian 09, Revision A.02.

Mafud, A.C., Silva, M.P.N., Monteiro, D.C., Oliveira, M.F., Resende, J.G., Coelho, M.L., De Sousa, D.P., Mendonça, R.Z., Pinto, P.L.S., Freitas, R.M., Mascarenhas, Y.P., De Moraes, J., 2016. Structural parameters, molecular properties, and biological

evaluation of some terpenes targeting Schistosoma mansoni parasite. Chem. Biol. Interact. 244, 129–139. https://doi.org/10.1016/j.cbi.2015.12.003.

Manley, P.W., Cowan-Jacob, S.W., Buchdunger, E., Fabbro, D., Fendrich, G., Furet, P., Meyer, T., Zimmermann, J., 2002. Imatinib: a selective tyrosine kinase inhibitor. Eur. J. Cancer 38 (Suppl 5), 19–27. https://doi.org/10.1016/s0959-8049(02)80599-8.

McManus, D.P., Dunne, D.W., Sacko, M., Utzinger, J., Vennervald, B.J., Zhou, X.N., 2018. Schistosomiasis. Nat. Rev. Dis. Prim. 4, 1–19. https://doi.org/10.1038/s41572-018-0013-8.

Mengarda, A.C., Mendonça, P.S., Morais, C.S., Cogo, R.M., Mazloum, S.F., Salvadori, M.C., Teixeira, F.S., Morais, T.R., Antar, G.M., Lago, J.H.G., de Moraes, J., 2020. Antiparasitic activity of piplartine (piperlongumine) in a mouse model of schistosomiasis. Acta Trop. 105350. https://doi.org/10.1016/j.actatropica.2020.105350.

Protasio, A.V., Tsai, I.J., Babbage, A., Nichol, S., Hunt, M., Aslett, M.A., de Silva, N., Velarde, G.S., Anderson, T.J.C., Clark, R.C., Davidson, C., Dillon, G.P., Holroyd, N.E., LoVerde, P.T., Lloyd, C., McQuillan, J., Oliveira, G., Otto, T.D., Parker-Manuel, S.J., Quail, M.A., Wilson, R.A., Zerlotini, A., Dunne, D.W., Berriman, M., 2012. A systematically improved high quality genome and transcriptome of the human blood fluke Schistosoma mansoni. PLoS Negl. Trop. Dis. 6. https://doi.org/10.1371/journal.pntd.0001455.

Race, P.R., Lovering, A.L., Green, R.M., Ossor, A., White, S.A., Searle, P.F., Wrighton, C.J., Hyde, E.I., 2005. Structural and mechanistic studies of Escherichia coli nitroreductase with the antibiotic nitrofurazone: reversed binding orientations in different redox states of the enzyme. J. Biol. Chem. 280, 13256–13264. https://doi.org/10.1074/jbc.M409652200.

Rajmane, S.V., Ubale, V.P., Lawand, A.S., Nalawade, A.M., Karale, N.N., More, P.G., 2013. A 4-(o-chlorophenyl)-2-aminothiazole: microwave assisted synthesis, spectral, thermal, XRD and biological studies. Spectrochim. Acta - Part A Mol. Biomol. Spectrosc. 115, 393–398. https://doi.org/10.1016/j.saa.2013.06.058.

Rana, K., Pandurangan, A., Singh, N., Tiwari, A.K., 2012. A systemic review of Schiff bases as an analgesic, anti-inflammatory. Acad. Sci. 4, 5–11.

Rando, D.G.G., da Costa, M.O.L., Pavani, T.F.A., Oliveira, T., dos Santos, P.F., Amorim, C.R., Pinto, P.L.S., de Brito, M.G., Silva, M.P.N., Roquini, D.B., de Moraes, J., 2019. Vanillin-related N-Acylhydrazones: synthesis, antischistosomal properties and target fishing studies. Curr. Top. Med. Chem. 19, 1241–1251. https://doi.org/10.2174/1568026619666190620163237.

Rodrigues, C.A., Freire, P., Oliveira, M., Fernanda, T., Pavani, A., Xander, P., Geraldo, M.M., Mengarda, A., Moraes, J.De, Gonçales, D., Rando, G., 2018. 4-Phenyl-1,3-thiazole-2-amines as scaffolds for new antileishmanial agents. J. Venom. Anim. Toxins Incl. Trop. Dis. 24, 1–10. https://doi.org/10.1186/s40409-018-0163-x.

Roquini, D.B., Cogo, R.M., Mengarda, A.C., Mazloum, S.F., Morais, C.S., Xavier, R.P., Salvadori, M.C., Teixeira, F.S., Ferreira, L.E., Pinto, P.L., Morais, T.R., Moraes, D., 2019. Promethazine exhibits antiparasitic properties in vitro and reduces worm burden, egg production, hepatomegaly, and splenomegaly in a Schistosomiasis. Anim. Model 63, 1–10. https://doi.org/10.1128/AAC.01208-19.

Silva, M.P., de Oliveira, R.N., Mengarda, A.C., Roquini, D.B., Allegretti, S.M., Salvadori, M.C., Teixeira, F.S., de Sousa, D.P., Pinto, P.L.S., da Silva Filho, A.A., de Moraes, J., 2017. Antiparasitic activity of nerolidol in a mouse model of schistosomiasis. Int. J. Antimicrob. Agents 50, 467–472. https://doi.org/10.1016/j.ijantimicag.2017.06.005.

World Health Organization, (2019) n.d. Schistosomiasis: Epidemiological situation [WWW Document]. URLhttps://www.who.int/schistosomiasis/epidemiology/en/ (accessed 2019).

Zabaleta, J., McGee, D.J., Zea, A.H., Hernández, C.P., Rodriguez, P.C., Sierra, R.A., Correa, P., Ochoa, A.C., 2004. Helicobacter pylori arginase inhibits T cell proliferation and reduces the expression of the TCR ζ-Chain (CD3ζ). J. Immunol. 173, 586–593. https://doi.org/10.4049/jimmunol.173.1.586.